A R C H I V E S O F M E T A L L U R G Y A N D M A T E R I A L S
Volume 59 2014 Issue 1
DOI: 10.2478/amm-2014-0005

A. GLOWACZ*, A. GLOWACZ**, P. KOROHODA***

RECOGNITION OF MONOCHROME THERMAL IMAGES OF SYNCHRONOUS MOTOR WITH THE APPLICATION OF BINARIZATION AND NEAREST MEAN CLASSIFIER

ROZPOZNAWANIE MONOCHROMATYCZNYCH OBRAZÓW TERMOWIZYJNYCH SILNIKA SYNCHRONICZNEGO Z ZASTOSOWANIEM BINARYZACJI I KLASYFIKATORA NAJBLIŻSZEJ ŚREDNIEJ

This article discusses the recognition method of imminent failure conditions of synchronous motor. The proposed approach is based on a study of thermal images of the motor. Studies were carried out for four conditions of motor with the application of binarization and nearest mean classifier with Manhattan distance. Pattern creation process used 40 monochrome thermal images. Identification process was carried out for 160 monochrome thermal images. The experiments show that the method can be useful for protection of synchronous motor. Moreover, this method can be used to diagnose equipments in steelworks and other industrial plants.

Keywords: Diagnostics, Recognition, Thermal images, Synchronous motor, nearest mean classifier

Artykuł omawia metodę rozpoznawania stanów przedawaryjnych silnika synchronicznego. Proponowane podejście jest oparte na badaniu obrazów termowizyjnych silnika. Przeprowadzono badania dla czterech stanów silnika z zastosowaniem binaryzacji i klasyfikatora najbliższej średniej z metryką Manhattan. Proces tworzenia wzorców do rozpoznawania został przeprowadzony dla 40 monochromatycznych obrazów termowizyjnych. W procesie identyfikacji użyto 160 monochromatycznych obrazów termowizyjnych. Eksperymenty pokazują, że metoda może być przydatna do ochrony silników synchronicznych. Ponadto metoda może być stosowana do diagnozowania urządzeń w hutach i innych zakładach przemysłowych.

1. Introduction

There have been many techniques over the past 40 years with infrared imaging. In 1800 William Herschel discovered infrared radiation when he was trying to measure the temperature of the separate colors of the rainbow spectrum cast on a table in the darkened room. He found the highest temperatures appear beyond the red end of the spectrum. Infrared radiation comprises the band between visible light and microwaves. All objects in the universe with a temperature greater than absolute zero emit radiations in the infrared region of the spectra as a function of their temperature. Thermal motion of charged particles in matter, causes thermal radiation. When an object gets hotter, it gives off more intense infrared radiation and it emits shorter wavelength [1]. Infrared thermography is the science of acquisition and analysis of infrared images. It is non-contact. Thermography also keeps the operator out of danger and does not affect investigated object. Infrared images can be analyzed. Human cannot see infrared rays below 700°C, but they can be detected by using the special devices for example infrared camera.

Electrical machines are constructed of steel elements. Thermal and mechanical properties of steel elements were investigated in the literature [2-7]. The article describes the method of diagnosis of a synchronous motor, based on recognition of thermal images.

2. Process of recognition of thermal images of synchronous motor

The process of recognition of thermal images contains two phases. First of them is pattern creation process (Fig. 1).

Second phase is identification process. These steps include algorithms used in image processing. At the beginning of pattern creation process movie is recorded in the computer memory. After that movie is converted into thermal images. Next binarization of the image is used. In next step sum of pixels values is calculated. Each sample which is used in pattern creation process gives us one sum of pixels values. Next all sums are averaged by nearest mean classifier (averaged feature vector). Steps of identification process are the same as

* AGH UNIVERSITY OF SCIENCE AND TECHNOLOGY, FACULTY OF ELECTRICAL ENGINEERING, AUTOMATICS, COMPUTER SCIENCE AND BIOMEDICAL ENGINEERING, DEPARTMENT OF AUTOMATICS AND BIOMEDICAL ENGINEERING, AL. MICKIEWICZA 30, 30-059 KRAKÓW, POLAND
** AGH UNIVERSITY OF SCIENCE AND TECHNOLOGY, FACULTY OF COMPUTER SCIENCE, ELECTRONICS AND TELECOMMUNICATIONS, DEPARTMENT OF TELECOMMUNICATIONS, AL. MICKIEWICZA 30, 30-059 KRAKÓW, POLAND
*** AGH UNIVERSITY OF SCIENCE AND TECHNOLOGY, FACULTY OF COMPUTER SCIENCE, ELECTRONICS AND TELECOMMUNICATIONS, DEPARTMENT OF ELECTRONICS, AL. MICKIEWICZA 30, 30-059 KRAKÓW, POLAND

for pattern creation process. Significant change occurs in the classification. In this step feature vectors are compared with each other (new feature vector and averaged feature vector).

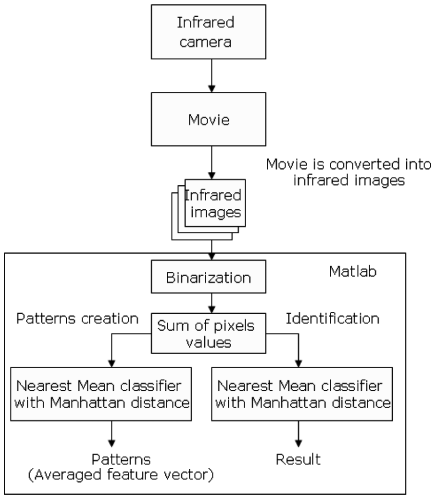

Fig. 1. Process of recognition of thermal image of synchronous motor with the use of binarization and nearest mean classifier

2.1. Video recording

All objects emit a certain amount of thermal radiation as a function of their temperatures. Generally the higher an object's temperature is, the higher is its emission. Thermal camera can detect this radiation in a way similar to a video camera recording visible light. It can work in darkness because it does not need an external light. Thermal camera used in experiments was installed 0.25m above rotor of synchronous motor. It recorded images at a resolution of PAL D-1 (720×576 pixels) in grayscale with a resolution of 8 bits (values 0-255). Next recorded video was transferred to a PC and stored in permanent memory in AVI format (Audio Video Interleave).

2.2. Binarization of thermal image

Binarization (thresholding) can be used to convert grayscale image into binary image. During the binarization process, some of pixels in an image form an object, if their value is greater than threshold value (assuming that an object is brighter than the background). This method of binarization is called *threshold above*. Opposite method of binarization is *threshold below*. Third method of binarization is *threshold inside*, where pixels form object when their values are between two thresholds and *threshold outside*, which is the opposite of *threshold inside*. Usually an object pixel has a value of 1 while a background pixel has a value of 0. In next step a binary image is created by coloring pixels white or black, depending on pixels values [8]. The key parameter in the binarization process is the choice of the threshold value. This parameter will be selected in the studies of the thermal images. Monochrome thermal images of rotor of synchronous motor were presented in Figures 2-5.

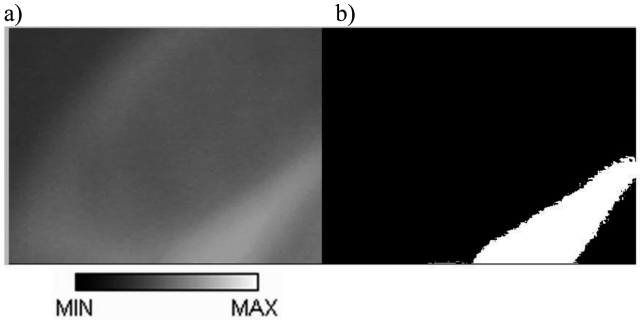

Fig. 2. a) Monochrome thermal image of rotor of faultless synchronous motor, b) Monochrome thermal image of rotor of faultless synchronous motor after binarization with threshold below equal to 0.6

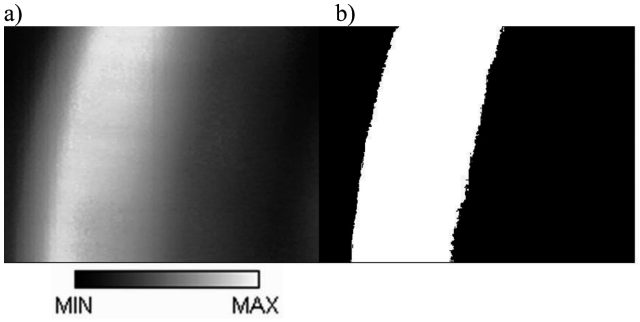

Fig. 3. a) Monochrome thermal image of rotor of synchronous motor with faulty ring of squirrel-cage, b) Monochrome thermal image of rotor of synchronous motor with faulty ring of squirrel-cage after binarization with threshold below equal to 0.6

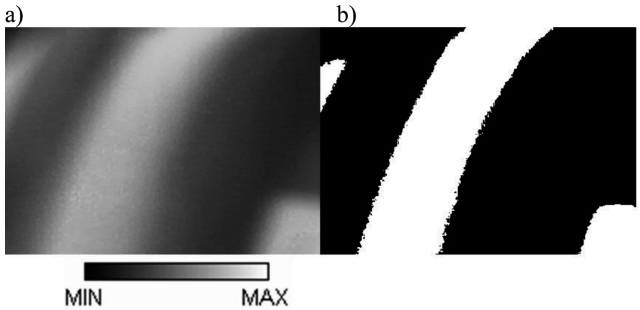

Fig. 4. a) Monochrome thermal image of rotor of synchronous motor with one faulty rotor bar, b) Monochrome thermal image of rotor of synchronous motor with one faulty rotor bar after binarization with threshold below equal to 0.6

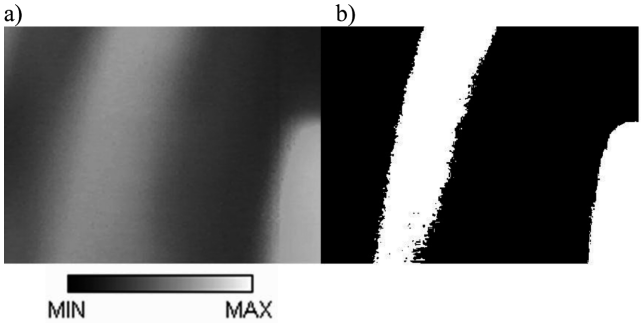

Fig. 5. a) Monochrome thermal image of rotor of synchronous motor with two faulty rotor bars, b) Monochrome thermal image of rotor of synchronous motor with two faulty rotor bars after binarization with threshold below equal to 0.6

2.3. Selection of features

Binary image contains 720×576 pixels. Each pixel has a value of 1 or 0 (0 – black pixel, 1 – white pixel). Feature of thermal image is the sum of all pixels values. Therefore, the feature vector will contain one feature (Fig. 6). This feature vector will be used in classification step.

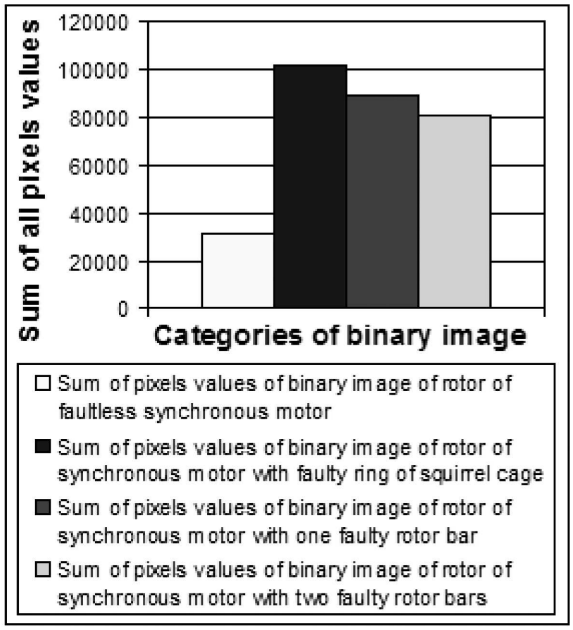

Fig. 6. Sums of pixels values for four categories of binary image

2.4. Nearest mean classifier

Different methods of classification of the signals were presented in the literature [9-25]. These algorithms are based on data processing. Nearest mean classifier is one of them. It is based on pattern creation process and identification process. Identification process uses training set and identification set. After binarization feature vector $\boldsymbol{x} = [x_1, x_2, \ldots, x_n]$ is obtained. Classes of patterns are defined as $w_1, w_2, \ldots w_M$, where M is the index number of the class. Averaged feature vectors $\mathbf{m_1}, \mathbf{m_2}, \ldots, \mathbf{m_j}$ are obtained in pattern creation process (1). These vectors form a training set.

$$\mathbf{m_j} = \frac{1}{P_j} \sum_{i=1}^{P_j} \mathbf{x_i} \tag{1}$$

where: $\mathbf{x_i} \in w_j$, P_j is the number of patterns from class w_j.

Feature vectors $\mathbf{y_1}, \mathbf{y_2}, \ldots, \mathbf{y_j}$ (sum of pixels values of selected thermal image) form identification set. After that minimum distance between feature vectors is obtained. For this purpose classifier uses Manhattan distance. This distance is given by following formula:

$$d(\mathbf{y}, \mathbf{m}) = \sum_{i=1}^{n} (|y_i - m_i|) \tag{2}$$

where: $\mathbf{y}$ and $\mathbf{m}$ are feature vectors with the same n lengths, $\mathbf{y}=[y_1, y_2, \ldots, y_n]$, $\mathbf{m}=[m_1, m_2, \ldots, m_n]$.

Finally thermal image is processed and recognized. Result of recognition of one image is *true* or *false*.

3. Results of thermal image recognition of synchronous motor

Investigations were carried out for three different failures of synchronous motor. They are denoted as follows: synchronous motor with faulty ring of squirrel-cage (Fig. 7), synchronous motor with one faulty rotor bar, synchronous motor with two faulty rotor bars. These failures did not cause the destruction of the machine.

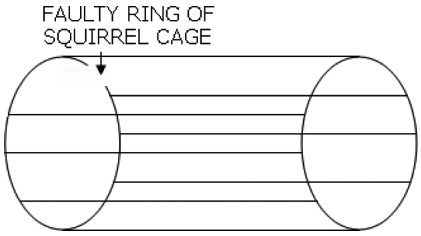

Fig. 7. Faulty ring of squirrel-cage of synchronous motor

Synchronous motor had following supply conditions: faultless synchronous motor, U = 300 V, I = 21.5 A, synchronous motor with faulty ring of squirrel-cage, U = 300 V, I = 77 A, synchronous motor with one faulty rotor bar, U = 300 V, I = 21 A, synchronous motor with two faulty rotor bars, U = 300 V, I = 20 A,

where: U – supply voltage, I – current of one motor phase.

Thermal camera recorded four movies. These movies contained thermal images of faultless synchronous motor and synchronous motors with failure.

The process of pattern creation was carried out for 40 monochrome thermal images. Identification process was carried out for 160 monochrome thermal images. Efficiency of thermal image recognition is defined as:

$$T = \frac{K_1}{K} \tag{3}$$

where: T – thermal image recognition efficiency, K_1 – number of correctly identified samples, K – number of all samples.

Efficiency of thermal image recognition of faultless synchronous motor was 100%. Efficiency of thermal image recognition of synchronous motor with faulty ring of squirrel-cage was 100%. Efficiency of thermal image recognition of synchronous motor with one faulty rotor bar was 100%. Efficiency of thermal image recognition of synchronous motor with two faulty rotor bars was 100%.

4. Conclusion

Thermography can be used for diagnostics of synchronous machines. The aim of this method is not to be a substitute for other techniques but to enhance them. There are many methods for temperature measurement. Non-contact temperature measurements are very good methods for small and inaccessible objects. High temperatures of the objects can be measured remotely. The method based on recognition of thermal images is non-invasive and non-radiating so, it can be

used without risk to the operator. Algorithms of data processing were investigated for synchronous motor. Results of thermal image recognition were good for binarization and nearest mean classifier with Manhattan distance. Efficiency of thermal image recognition of synchronous motor was 100%. Further researches should be continued to examine other failures of electrical machines and metallurgical equipment.

Acknowledgements

The work of Adam Głowacz has been supported by the AGH University of Science and Technology under contractno. 11.11.120.612.

The work of Andrzej Głowacz has been supported by the AGH University of Science and Technology under contract no.11.11.230.018.

REFERENCES

[1] H. Qi, P.T. Kuruganti, Detecting Breast Cancer from Thermal Infrared Images by Asymmetry Analysis, Medicine and Medical Research, 38 pages (2003).

[2] M. Florkowski, J. Furgal, M. Kuniewski, Impact of transformers from overvoltages transferred through windings, Przeglad Elektrotechniczny **88**, 5A, 104-107 (2012).

[3] Z. Glowacz, J. Kozik, Feature selection of the armature windings short circuit fault in synchronous motor using genetic algorithm and the Mahalanobis distance, Przeglad Elektrotechniczny **88**, 2, 204-207 (2012).

[4] W. Orlewski, A. Siwek, Hydroelectric power plant using dump industrial water, Rynek Energii **6**, 87-91 (2010).

[5] O.A. Kogtenkova, S.G. Protasova, A.A. Mazilkin, B.B. Straumal, P. Zięba, T. Czeppe, B. Baretzky, Heat effect of grain boundary wetting in Al-Mg alloys, Journal of Material Science **47**, 24, 8367-8371 (2012).

[6] J. Tomczak, Z. Pater, T. Bulzak, Effect of technological parameters on the rotary compression process, Eksploatacja i Niezawodność – Maintenance and Reliability **15**, 3, 279-283 (2013).

[7] Z. Gronostajski, M. Hawryluk, J. Krawczyk, M. Marciniak, Numerical modelling of the thermal fatigue of steel WCLV used for hot forging dies, Eksploatacja i Niezawodność – Maintenance and Reliability **15**, 2, 129-133 (2013).

[8] L.G. Shapiro, G.C. Stockman, Computer Vision 2002, Prentice Hall, ISBN 0-13-030796-3.

[9] E. Kantoch, M. Smolen, P. Augustyniak, P. Kowalski, Wireless Body Area Network System based on ECG and Accelerometer Pattern, IEEE Conference on Computing in Cardiology, Hangzhou, China, 245-248 (2011).

[10] T. Orzechowski, A. Izworski, R. Tadeusiewicz, K. Chmurzynska, P. Radkowski, I. Gatkowski, Processing of pathological changesin speech caused by dysarthria, Proceedings of ISPACS 2005, IEEE International Symposium on Intelligent Signal Processing and Communication Systems-ISPACS, 49-52 (2005).

[11] D. Gogola, A. Krafcik, O. Strbak, I. Frollo, Magnetic Resonance Imagingof Surgical Implants Made from Weak Magnetic Materials, Measurement Science Review **13**, 4, 165-168 (2013).

[12] M. Michalak, M. Sikora, J. Sobczyk, Analysis of the longwall conveyor chain based on a harmonic analysis, Eksploatacja i Niezawodność – Maintenance and Reliability **15**, 4, 332-336 (2013).

[13] H. Piotrzkowska, J. Litniewski, E. Szymanska, A. Nowicki, Ultrasonic Echosignal Applied to Human Skin Lesions Characterization, Archives of Acoustics **37**, 1, 103-108 (2012).

[14] R. Olszewski, Z. Trawinski, J. Wojcik, A. Nowicki, Mathematical and Ultrasonographic Model of the Left Ventricle: in Vitro Studies, Archives of Acoustics **37**, 4, 583-595 (2012).

[15] K. Skowronek, A. Wozniak, FFT-PCA-LDA classifier in A.C. Generator diagnostics, Eksploatacja i Niezawodność – Maintenance and Reliability **15**, 2, 140-146 (2013).

[16] J. Girtler, M. Slezak, Four-state stochastic model of changes in the reliability states of a motor vehicle, Eksploatacja i Niezawodność – Maintenance and Reliability **15**, 2, 165-160 (2013).

[17] T. Hachaj, M.R. Ogiela, Application of neral networks in detection of abnormal brain perfusion regions, Neurocomputing **122** (Special Issue), 33-42 (2013).

[18] J. Jaworek, P. Agustyniak, A cardiac telerehabilitation application for mobile devices, IEEE Conference on Computing in Cardiology, Hangzhou, China 241-244 (2011).

[19] T. Kryjak, M. Gorgon, Pipeline Implementation of Peer Group Filtering in FPGA, Computing and Informaties **31**, 4, 727-741 (2012).

[20] M. Trzupek, M.R. Ogiela, R. Tadeusiewicz, Intelligent image content semantic description for cardiac 3D visualisations, Engineering Applications of Artificial Intelligence **24**, 8, 1410-1418 (2011).

[21] P. Mishra, S.K. Singla, Artifact Removal from Biosignal using Fixed Point ICA Algorithm for Preprocessing in Biometric Recognition, Measurement Science Review **13**, 1, 7-11 (2013).

[22] T. Pieciak, bootstrap Uncertainty Estimation of Canine Cardiac Fibers Anisotropy and Diffusivity on DT-MRI Data, IEEE 39th Conference on Computing in Cardiology, Book Series: Computers in Cardiology Series **39**, 369-372 (2012).

[23] M. Tomala, T. Miszalski-Jamka, W. Zajdel, A. Chrustowicz, K.K. Grobler-Dębska, K. Zmudka, Right ventricular infarction: right ventricular branch compromise after primary percutancous coronary intervention in inferior myocardial infarction is the key predictor of poor right ventricular, European Heart Journal **33**, Supplement: 1, 1016-1017 (2012).

[24] S. Duda, Numerical modeling and simulating the dynamic interactions within the drive system of electric rail vehicles, Eksploatacja i Niezawodność – Maintenance and Reliability **15**, 4, 343-348 (2013).

[25] C. Zhang, S. Wang, Solid lubricated bearings performance degradation assessment: A fuzzy selforganizing map method, Eksploatacja i Niezawodność – Maintenance and Reliability **15**, 4, 397-402 (2013).

Received: 10 May 2013.